International Journal of Minerals, Metallurgy and Materials
Volume 21, Number 4, April 2014, Page 317
DOI: 10.1007/s12613-014-0911-z

Influence of acid leaching and calcination on iron removal of coal kaolin

Pei-wang Zhu, Wei-qiang Zeng, Xiu-lin Xu, Le-ming Cheng, Xiao Jiang, and Zheng-lun Shi

State Key Laboratory of Clean Energy Utilization, Zhejiang University, Hangzhou 310027, China

(Received: 23 October 2013; revised: 17 December 2013; accepted: 19 December 2013)

Abstract: Calcination and acid leaching of coal kaolin were studied to determine an effective and economical preparation method of calcined kaolin. Thermogravimetric–differential thermal analysis (TG–DTA) and X-ray diffraction (XRD) demonstrated that 900°C was the suitable temperature for the calcination. Leaching tests showed that hydrochloric acid was more effective for iron dissolution from raw coal kaolin (RCK), whereas oxalic acid was more effective on iron dissolution from calcined coal kaolin (CCK). The iron dissolution from CCK was 28.78wt%, which is far less effective than the 54.86wt% of RCK under their respective optimal conditions. Through analysis by using Mössbauer spectroscopy, it is detected that nearly all of the structural ferrous ions in RCK were removed by hydrochloric acid. However, iron sites in CCK changed slightly by oxalic acid leaching because nearly all ferrous ions were transformed into ferric species after firing at 900°C. It can be concluded that it is difficult to remove the structural ferric ions and ferric oxides evolved from the structural ferrous ions. Thus, iron removal by acids should be conducted prior to calcination.

Keywords: kaolin; iron removal; calcination; acid leaching; extraction; Mössbauer spectroscopy

1. Introduction

Coal kaolin, coal gangue dominated by kaolin, is widely deposited in China, and it is estimated that the amount up to 11.09 billion tons has been deposited in reserves [1]. Because coal gangue is generated simultaneously with the production of coal, the strong demand for coal in China over the last decades has resulted in a considerable increase in coal gangue waste [2]. It has been estimated that 4.5 billion tons of coal gangue are stockpiled at 1700 waste dumps occupying 15000 hectares of land [3]. Consequently, the waste takes up large areas of land, which results in water and soil pollution, soil erosion, and other environmental problems [4–5]. The disposal of this coal wastes has turned out to be an increasing economic and environmental burden because of the increasing regulatory laws and the increasing costs of landfill expenses [6].

To minimize the waste of resources and to protect the environment, many researchers have focused on alternative utilization of coal gangue. The main ingredients of coal gangue are carbonaceous and clay minerals, which can be used as raw industrial materials. Beneficial uses of coal gangue include power generation [7] and original substances for construction materials such as cement, bricks, and concrete [8–9]. However, the utilization rate of coal gangue in cement as an admixture is always lower than 15% because of its weak cementitious capability [10]. In addition, a large amount of valuable mineral resources such as SiO_2, Al_2O_3, Fe_2O_3, CaO, and other oxides existing in the coal gangue can be extracted as beneficial materials for value-added products. Mesoporous Al_2O_3, calcined kaolin/TiO_2 composite particle material (CK/TCPM), and porous ceramics have been successfully synthesized from coal kaolin [11–13].

For large-scale utilization of coal gangue, kaolin products have been examined by many researchers. When used for kaolin products, the coal gangue must meet the required thermal stability and whiteness [14]. Therefore, research has been conducted on two procedures: calcination and iron removal.

Cheng *et al.* [15] investigated the thermal transformation of coal kaolinite by thermogravimetric analysis–mass spectrometry (TG–MS) and infrared emission spectroscopy. Results show that after calcination, some kaolinite structures

Corresponding author: Zheng-lun Shi E-mail: szl@zju.edu.cn

break down, and the iron-containing minerals are converted to free oxides that impart color to the product. The minimum brightness occurs from 500°C to 600°C for kaolin samples, whereas a sharp improvement in optical properties for all the samples from 1000°C to 1100°C agrees well with the crystallization of mullite, as indicated by the XRD studies [16]. In addition, after calcining coal kaolin from Jiaozuo at 900°C for 4 h with a 5wt% reducing agent and a 2wt% chlorinating agent, the whiteness of the kaolin product increased from 45.84wt% to 88.68wt% and satisfied the demands for rubber filling and moderating paper coating [17].

The main contaminant in clay and kaolin minerals is iron, which is negatively related to lightness [18]. Leaching studies have been performed for iron removal that employed various chemicals such as oxalic acid, hydrochloric acid, citric acid, carbohydrates, and ascorbic acid [19–21]. For oxalic acid, Ambikadevi and Lalithambika [22] reported that the optimum conditions required for achieving brightness ≥ 80% are a temperature of 100°C, an oxalic acid concentration of 0.1 mol/L, and a reaction time of 90 min. Oxalic–sulphuric acid treatments showed better iron extraction yields than that when sulphuric acid was used alone [21]. On the other hand, physical methods such as flocculation and high-gradient magnetic separation also achieved good performances [23–25].

In these methods, chemical processing to remove the contaminated iron oxides from clay and silica minerals was considered as the most cost-efficient method [26]. In the present investigation, iron dissolution from coal kaolin by hydrochloric and oxalic acids is studied before and after calcination. Factors such as acid concentration, temperature, reaction time, and solid-to-liquid ratio (S/L) are examined to achieve reasonable conditions. The residues of coal kaolin are characterized by XRD and ^{57}Fe Mössbauer spectroscopy to probe the impacts of acid leaching and calcination on iron removal and the phase of ferrum that were not presented in previous studies and to provide insight into future coal kaolin processing.

2. Experimental

2.1. Raw materials

Raw coal kaolin (RCK) used in this study was obtained from northeast China. The sample was crushed to pass through a 0.074 μm sieve for analysis, and moisture was removed by placing the sample in a desiccator after drying at 105°C and self-cooling. Table 1 shows that the chemical and mineralogical compositions were tested by XRD and inductively coupled plasma optical emission spectrometer (ICP–OES) analysis. It is evident that the major phases of RCK are kaolinite and quartz minerals; however, the quantity of iron present demonstrates that RCK is highly contaminated. The valence states of iron were tested by Beijing General Research Institute of Mining and Metallurgy.

Table 1. Chemical and mineral characteristics of the coal kaolin sample

Category	Component	Content / wt%
Chemical composition	SiO_2	36.75
	Al_2O_3	25.66
	Fe_2O_3	3.44
	CaO	0.25
	MgO	0.71
	K_2O	0.38
	Na_2O	0.24
	TiO_2	0.89
	Loss on ignition*	31.24
Valence state of iron	Fe^{2+} in RCK	71.86
	Fe^{3+} in RCK	28.14
	Fe^{2+} in CCK	17.39
	Fe^{3+} in CCK	82.61
Minerals	Kaolinite	
	Quartz	

Note: *—Calcining at a temperature of 900°C.

Hydrochloric acid (37wt%) was obtained by the Hangzhou Chemical Reagent Company. Other analytical grade reagents including oxalic acid, sodium acetate, glacial acetic acid, hydroxylamine hydrochloride, and phenanthroline were obtained by Sinopharm Chemical Reagent Co., Ltd.

2.2. Thermal analysis

To observe the changes in the physical properties of RCK during thermal treatment, the RCK sample was placed in an STA449 F3 thermal analysis system for TG–DTA. The 10-mg sample underwent thermal treatment with a linear heating rate of 10°C/min, from 20°C to 1300°C, in a flowing air atmosphere (60 mL/min). Typical temperature points of 600, 700, 800, 900, 1000, 1100, and 1200°C were selected to analyze the mineral composition by calcining coal kaolin with a muffle roaster. Each sample was heated for 2 h and then cooled down in a dryer.

2.3. Leaching studies

As indicated in Table 1, due to calcination the Fe^{3+} and Fe^{2+} contents resulted in significant differences in RCK and calcined coal kaolin (CCK). Iron leaching tests were con-

ducted by two different methods. The first method involved the use of hydrogen chloride to leach iron from RCK, and the other involved the use of oxalic acid to leach iron from CCK.

Leaching tests were conducted in a 50-mL glass beaker that was placed on a magnetic hot plate for heating and stirring. The speed of agitation was constant to ensure suspension of the particles. The leaching agents were prepared at desired concentrations by dissolving known masses or volumes of acids in distilled water. Thus, the variables that affect coal kaolin bleaching and iron leaching are temperature, acid concentration, S/L, and duration of the process.

2.4. Characterization and evaluation

The iron leached from the kaolin was measured by using the 1, 10-phenanthroline colorimetric method. Other elements including Si and Al were tested according to the China Standard: GB/T 14563—2008 specification and test method of kaolin clay. X-ray analysis was performed by the Rigaku D/Max–2550pc powder diffractometer, using Cu K_α (λ = 0.154059 nm) radiation at 40 kV and 250 mA. The scans were run from 5° to 85.0° (2θ), with an increasing step size of 0.02° and a scan rate of 5°/min. Data were processed by using MDI–Jade version 7.0 software.

^{57}Fe Mössbauer spectra were recorded at room temperature with a standard constant acceleration spectrometer by using a ^{57}Co/Pd source. The velocity scale (±10 mm/s) was calibrated with a standard α-Fe foil, and all isomer shifts were given with respect to the center of the α-Fe spectrum. The 1.5-g samples were placed in a 2-mm-thick holder and were prepared as absorbers. The entire spectral Mössbauer parameters were fitted to Lorentzian lines by a least-squares method that used the ISO fit programme [27]. The various phases of iron in the samples were determined by comparing the Mössbauer parameters with the previous results [28–31]. Quantitative phase identification of iron in the samples was calculated with reference to the Huffman method [28].

3. Results and discussion

3.1. Mineral and thermal characterization

The weight loss TG–DTA curves as the functions of the temperature of RCK are illustrated in Fig. 1. In the first stage of the endothermic reaction, the mass loss from 20°C to 100°C was 3wt% because of the loss of surface water, bound water, and void water. From 100°C to 275°C, a net weight gain of 1wt% was recorded, which is attributed to oxygen chemisorptions occurring prior to the onset of combustion [32]. The second stage from 275°C to 654°C was exothermic and showed a significant mass loss of up to 29wt% of the sample. The mass of the sample then became stable. This major mass loss and intense exothermicity is because of the combustion of organic matter and carbon.

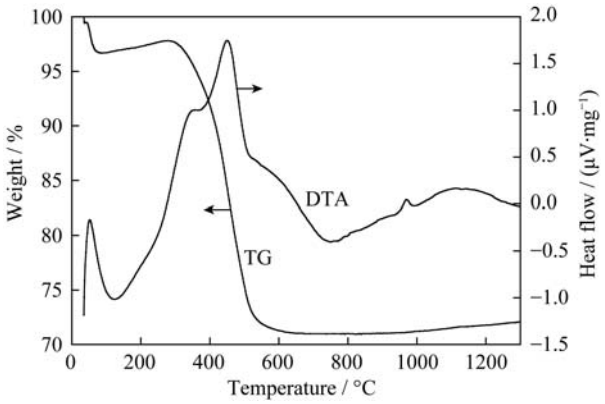

Fig. 1. Thermogravimetric–differential thermal analyzer (TG–DTA) curves of coal kaolin under air atmosphere.

Fig. 2 shows that the structure lost its crystallographic order between 500°C and 900°C when compared with RCK, the mineral phases of which are kaolinite, quartz, and dickite. Moreover, new diffraction peaks occurred because of the generation of crystals such as hematite and silicon. The dominant mineral in RCK altered to metakaolin. Dehydroxylation continued up to 963°C, and the gradual oxolation of the metakaolin generated a complex amorphous structure of aluminum–silicon spinel ($Si_3Al_4O_{12}$) [33]. These reactions contributed to a weak endothermic effect. With an increase in temperature, an inconspicuous exothermic effect reappeared because the amorphous substance nucleated and formed mullite ($3Al_2O_3{\cdot}2SiO_2$) crystals and highly crystalline cristobalite (SiO_2). However, the formation of these minerals is a disadvantage to the product of calcined kaolin. Therefore, the coal kaolin calcined at 900°C was selected for leaching with oxalic acid.

3.2. Leaching RCK by hydrochloric acid

Previous orthogonal experiments indicated that hydrogen chloride was more suitable for leaching iron from RCK. Leaching tests with RCK by hydrochloric acid were conducted with various acid concentrations, reaction temperatures, time, and S/L. The effect of one factor on iron removal was obtained while keeping other factors constant. Fig. 3(a) shows the effect of acid concentration on iron dissolution while maintaining 20°C for 2 h and an S/L of 1 g : 4 mL. It was observed that with the increase of acid concentration, the dissolution of iron increased until the acid concentration was 2.0 mol/L. Beyond this concentration, the effect was less significant. Thus, the iron leaching rate of

48.43wt% was achieved as the maximum value. It can be suggested that an increase in hydrochloric acid results in higher cost and does not always lead to better performance of the iron leaching rate.

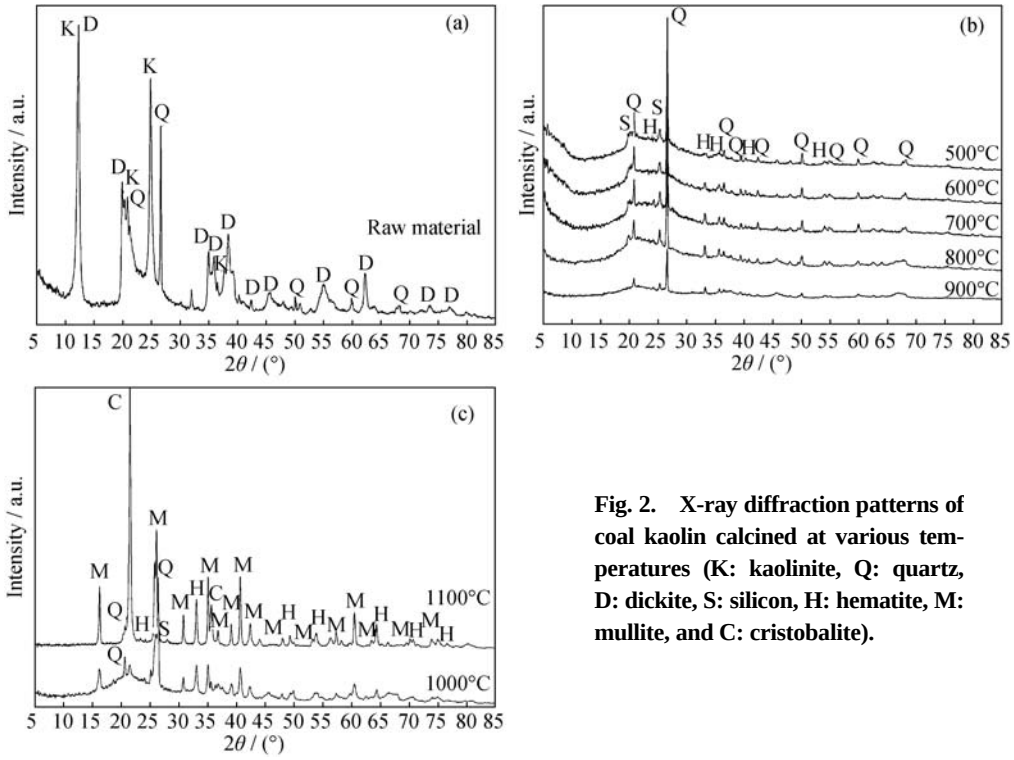

Fig. 2. X-ray diffraction patterns of coal kaolin calcined at various temperatures (K: kaolinite, Q: quartz, D: dickite, S: silicon, H: hematite, M: mullite, and C: cristobalite).

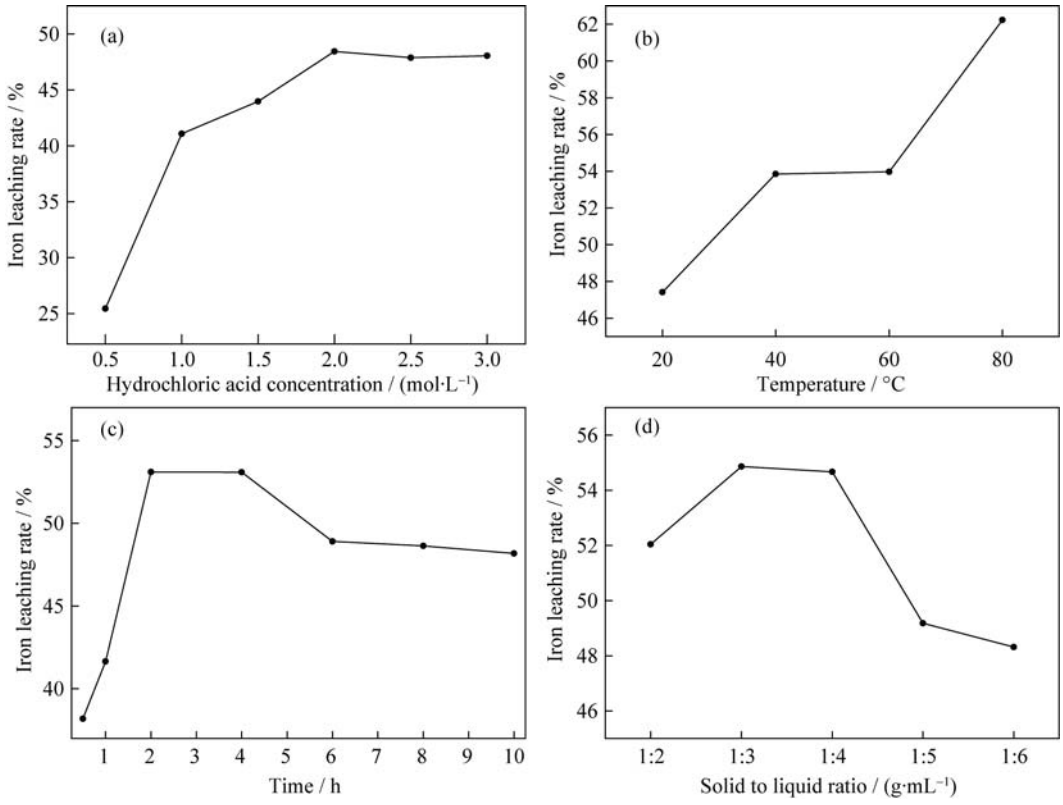

Fig. 3. Effects of hydrochloric acid on iron dissolution from raw coal kaolin (RCK): (a) effect of acid concentration at 20°C and an S/L of 1 g : 4 mL for 2 h; (b) effect of temperature at 2.0 mol/L and an S/L of 1 g : 4 mL for 2 h; (c) effect of reaction time at 2.0 mol/L, 40°C, and an S/L of 1 g : 4 mL; (d) effect of S/L at 2.0 mol/L and 40°C for 2 h.

Fig. 3(b) illustrates the increase in the iron leaching rate with an increase in temperature. The constant factors were 2.0 mol/L hydrochloric acid, 2 h, and an S/L of 1 g : 4 mL. Results show the dissolution of iron was slow and varied between 40°C and 60°C. Two stages of rapid increase in the iron leaching rate were observed including that from 20°C to 40°C and from 60°C to 80°C. These results indicate that the increased temperature contributes to a swelling effect within the internal structure of RCK, which improves the reaction activity of the iron leaching. However, the component analysis of the leaching residues indicates that aluminum dissolution at 60°C is 6.47wt%, which is significantly higher than 1.07wt% corresponding to that of 40°C. These conditions are harmful to the kaolin product; therefore, 40°C was selected for the temperature in the following leaching tests.

Fig. 3(c) shows the dissolution of iron at various times with 2.0 mol/L hydrochloric acid at 40°C and an S/L of 1 g : 4 mL. During the first half of the experiment time, the dissolution of iron increased rapidly, and a maximum iron leaching rate of 53.1wt% at 2 h was achieved. The slow decrease in iron leaching rate indicates that the particle surface may have been blocked by a product layer. It can be concluded that 2 h is suitable for iron leaching from RCK by hydrochloric acid.

Changes in the S/L had a limited effect on the dissolution of iron from RCK, as shown in Fig. 3(d). Tests were conducted under the conditions of 2.0 mol/L hydrochloric acid at 40°C with a 2 h reaction time. In the range from 1 g : 2 mL to 1 g : 6 mL, the dissolution of iron had a small change within 6wt%. However, the iron leaching rate affected by S/L appeared to show a clear trend, such that the dissolution of iron increased with S/L after the first cut increased. When S/L was 1 g : 3 mL, the maximum iron leaching rate was 54.86wt%.

In this work, suitable conditions for the RCK iron leaching process were achieved, which are 2.0 mol/L hydrochloric acid at 40°C with a 2 h reaction time and an S/L of 1 g : 3 mL.

3.3. Leaching CCK by oxalic acid

Before leaching CCK by oxalic acid, a comparative leaching test was conducted on CCK by hydrochloric acid under the suitable conditions achieved in the previous section. The results show that the dissolution of iron was only 11.76wt%, which is undesirable. However, ferric ion can form a stable water-soluble chelate with oxalic acid. Lee *et al.* [34] reported that oxalic acid was the most promising solvent reagent because of its acid strength, good complexing characteristics, and high reducing power over those of other organic acids. Hence, oxalic acid was examined to determine an optimum condition of higher iron dissolution from CCK.

First, tests were conducted to establish the iron dissolution with oxalic acid concentration at room temperature (20°C) and an S/L of 1 g : 3 mL. Fig. 4(a) shows the results of dissolution over a period of 16 h. The iron dissolution was independent of the oxalic acid concentration from 0.05 to 1 mol/L, although the dissolution rate did increase when the oxalic acid concentration increased during the early stage. However, the trends in iron leaching rates varied with time. From 0.05 to 0.5 mol/L, the iron leaching rate first increased with an increase in reaction time. When the reaction time reached 8 h, the maximum value was obtained, and the iron dissolution rate then decreased. This result indicates that a long reaction time causes side effects in iron dissolution. At 1.00 mol/L, the iron dissolution continued to decrease over 16 h, which demonstrates that lengthy reaction time and high oxalic acid concentration are harmful to iron dissolution from CCK. The reasonable conditions at room temperature were determined to be 0.1 mol/L oxalic acid concentration at 8 h for the maximum iron dissolution of 28.78%.

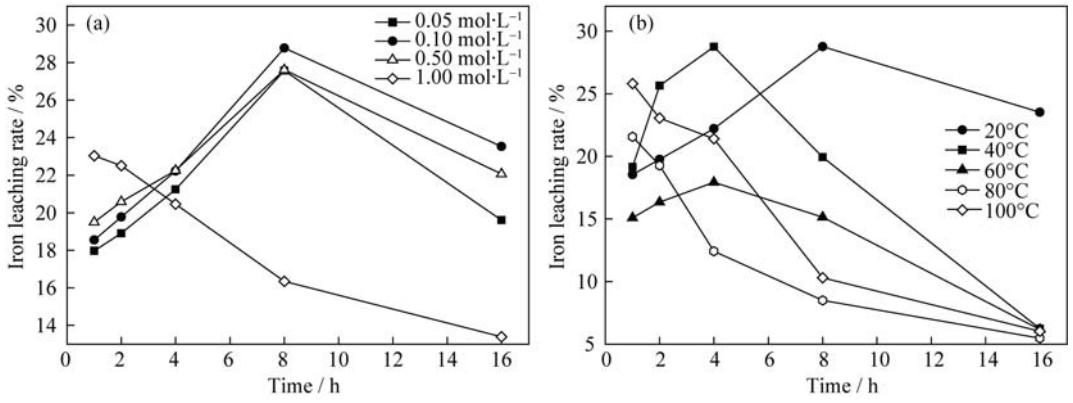

Fig. 4. Effects of oxalic acid on iron dissolution from calcined coal kaolin (CCK): (a) effect of acid concentration at 20°C; (b) effect of temperature at 0.1 mol/L acid concentration.

Fig. 4(b) shows the effects of temperature on iron dissolution over time while maintaining an oxalic acid concentration of 0.1 mol/L. At lower temperatures below 60°C, the removal of iron increased with an increase in reaction time before gradually decreasing. The maximum point of iron dissolution always occurred from 1 to 16 h. At 20°C, the maximum point of iron dissolution was 28.78wt% at 8 h. For 40°C, it was 28.75wt% at 4 h, and for 60 °C it was 17.93wt% at 4 h. At higher temperatures above 60°C, iron dissolution decreased from the maximum to minimum levels with an increase in reaction time. The results observed in Fig. 4(b) illustrate that high temperature enhanced iron dissolution whereas lengthy reaction time restricted iron dissolution, causing the maximum iron dissolution shift to a lower reaction time with temperature increase.

In these tests, the effect of iron dissolution at 40°C in 4 h was approximately the same as that at 20°C in 8 h. Both are suitable conditions for iron removal by 0.1 mol/L oxalic acid. Moreover, leaching of CCK by oxalic acid obtained an iron leaching rate of 28.78wt%, which is better than that by hydrochloric acid at 11.76wt%.

Finally, a contrast test was conducted to examine the effects of iron dissolution from RCK by oxalic acid under the determined suitable conditions of 40°C and 4 h reaction time. The results show that the iron leaching rate reached 49.84wt%, which is less than that by hydrochloric acid at 54.86wt%, and confirms that hydrochloric acid is better for iron dissolution from RCK.

3.4. Product analysis by Mössbauer spectroscopy studies

Four samples were investigated to demonstrate the effects of calcination, hydrochloric acid, and oxalic acid on iron distribution in kaolin through Mössbauer spectroscopy, which provided information on iron site geometry and iron valence [35]. RCK, CCK, and coal kaolin processed by hydrochloric acid (CKHA) and CCK processed by oxalic acid (CCKO) obtained from the above experiments were used under their respective optimal conditions.

Fig. 5 shows the Mössbauer spectra of the four samples at room temperature. In Fig. 5(a), the Mössbauer spectrum of RCK consists of a doublet and a singlet with two different isomer shifts (IS) and quadrupole splitting (QS). The doublet with IS = 1.002 mm/s and QS = 2.123 mm/s can be associated with Fe^{III}, which may substitute for Al^{III} in kaolinite. The singlet, with IS = 1.16 mm/s and QS = 2.85 mm/s, corresponds to the dominant part of iron and could be related to structural ferrous ions. The iron contents of the four samples (Table 2) were calculated from the relative surfaces of their respective subspectra, which are referred to as atom quantities.

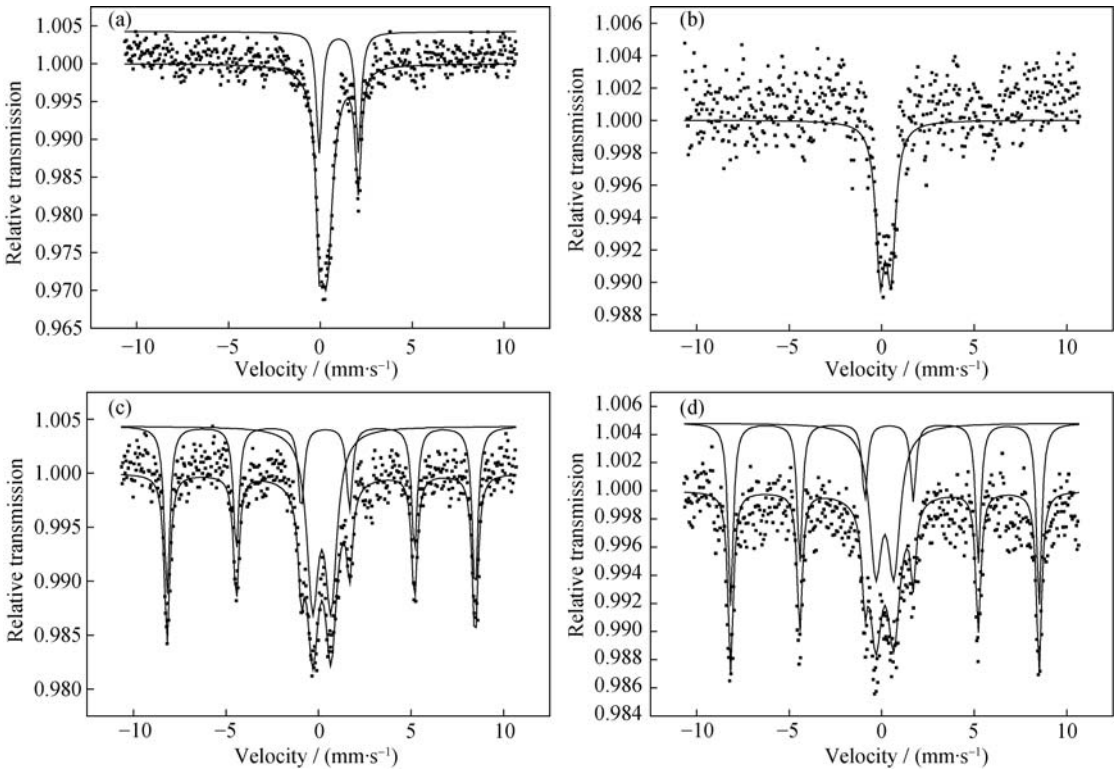

Fig. 5. Mössbauer spectra of kaolin samples at room temperature: (a) raw coal kaolin (RCK); (b) coal kaolin processed by hydrochloric acid (CKHA); (c) calcined coal kaolin (CCK); (d) calcined coal kaolin processed by oxalic acid (CCKO).

Table 2. Mössbauer parameters of iron-bearing phases in four samples at room temperature

Sample	IS / (mm·s^{-1})	QS / (mm·s^{-1})	MHF / T	Assignment	Content / wt%
RCK	0.341	—	—	Fe^{II}	64.064
	1.002	2.123	—	Fe^{III}	35.936
CKHA	0.212	0.584	—	Fe^{III}	100
CCK	0.256	−0.116	51.923	Iron oxides	51.571
	0.182	0.994	—	Fe^{III}	48.729
CCKO	0.282	−0.112	51.993	Iron oxides	54.606
	0.168	0.980	—	Fe^{III}	45.394

Fig. 5(b) shows the Mössbauer spectrum of CKHA. It is composed only of one doublet with IS = 0.212 mm/s and QS = 0.584 mm/s, which corresponds to Fe^{III}. That is, after leaching by hydrochloric acid, the Fe^{II} species in RCK was effectively removed. However, the Fe^{III} in kaolinite is not easily dissolved by hydrochloric acid.

After heating at 900°C for 2 h, additional sextets appeared in CCK (Fig. 5(c)) that led to a magnetic hyperfine field (MHF) of 51.923 T with IS = 0.256 mm/s and QS = −0.116 mm/s. The ferrous cells trapped within the normal dioctahedral aluminum structure then transformed into Fe^{3+} species. When the Fe^{II} disappeared, the hematite and magnetic irons increased according to the magnetically split sextets. Theoretically, the content of Fe^{III} will decrease because high temperature leads to a partial collapse of the kaolinite crystal, which contributes to the transformation of Fe^{III} into iron oxide. In fact, Table 2 shows an increase. Thus, some octahedral Fe^{II} must have transformed into Fe^{III} octahedral species, which increased the difficulty of iron removal.

After processing by oxalic acid, the chemical treatment did not significantly influence the line profiles of the Mössbauer spectrum (Fig. 5(d)). The iron distributions of CCKO also changed slightly compared to those of CCK. From Table 2, it can be inferred that the relative content of Fe^{III} in CCKO decreased compared to that of Fe^{III} in CCK. This result indicates that at least small parts of Fe^{III} were dissolved.

The spectroscopy study demonstrates the adverse effects of calcination on iron removal. Because of the calcination process, nearly all ferrous ions changed into ferric species, which caused lower iron dissolution by chemical treatment. For this reason, the iron leaching rate from CCK (28.78wt%) is significantly less effective than that of RCK (54.86wt%) under their respective optimal conditions.

4. Conclusions

TG–DTA and XRD analysis were conducted to determine a suitable temperature for calcined kaolin preparation. Two chemical methods were then proposed for iron removal to study whether acid leaching before or after calcination was more effective. Reasonable conditions for each process were obtained through many experiments with the variables of concentration, reaction temperature, and time. The raw materials and products were analyzed by Mössbauer spectroscopy to determine the effects of calcination and acid leaching on the iron distribution of RCK. The following conclusions were drawn:

(1) 900°C is a suitable temperature for the calcination of RCK. Below 900°C, conditions are unfavorable for decarburization; those over 900°C cause the formation of mullite and cristobalite, which is detrimental to the kaolin product.

(2) With regard to RCK leaching by hydrochloric acid, the maximum iron leaching rate (54.86wt%) was achieved under the conditions of 2 mol/L hydrochloric acid at 40°C with a 2 h reaction time and an S/L of 1 g : 3 mL.

(3) For CCK, the effect of iron dissolution (28.75wt%) at 40°C in 4 h was approximately the same as that at 20°C for 8 h (28.78wt%). 0.1 mol/L oxalic acid was used for both conditions.

(4) Mössbauer spectroscopy showed that nearly all of the structural ferrous ions in RCK were removed by acids. However, iron sites in CCK altered slightly after processing by oxalic acid because nearly all ferrous ions were transformed into ferric species after firing at 900°C.

(5) The structural ferric ions and ferric oxides evolved from ferrous ions by acids were difficult to remove; therefore, iron removal by acids should be achieved prior to calcination.

Acknowledgements

The study is financially supported by Zhejiang Natural Science Foundation (No. Y1080393) and Opening Foundation of State Key Laboratory of Clean Energy Utilization (No. ZJUEDU2012001). We are grateful to Mr. Tong Jian-

chun at Department of Energy Engineering, Zhejiang University, for the help in the measurement of coal kaolin.

References

[1] Z.G. Wu, S.L. Shi, and Q.F. Liu, Preparation of micro-porous calcium silicate with coal series kaolin, *Met. Mine*, (2011), No. 1, p. 162.

[2] H.B. Liu and Z.L. Liu, Recycling utilization patterns of coal mining waste in China, *Resour. Conserv. Recycl.*, 54(2010), No. 12, p. 1331.

[3] Z.F. Bian, J.H. Dong, S.G. Lei, H.L. Leng, S.G. Mu, and H. Wang, The impact of disposal and treatment of coal mining wastes on environment and farmland, *Environ. Geol.*, 58(2009), No. 3, p. 625.

[4] J.D.N. Pone, K.A.A. Hein, G.B. Stracher, H.J. Annegarn, R.B. Finkleman, D.R. Blake, J.K. McCormack, and P. Schroeder, The spontaneous combustion of coal and its by-products in the Witbank and Sasolburg coalfields of South Africa, *Int. J. Coal. Geol.*, 72(2007), No. 2, p. 124.

[5] G.B. Stracher and T.P. Taylor, Coal fires burning out of control around the world: thermodynamic recipe for environmental catastrophe, *Int. J. Coal. Geol.*, 59(2004), No. 1-2, p. 7.

[6] L. Barbieri, I. Lancellotti, T. Manfredini, G.C. Pellacani, J.M. Rincòn, and M. Romero, Nucleation and crystallization of new glasses from fly ash originating from thermal power plants, *J. Am. Ceram. Soc.*, 84(2001), No. 8, p. 1851.

[7] Y.P. Chugh and A. Patwardhan, Mine-mouth power and process steam generation using fine coal waste fuel, *Resour. Conserv. Recycl.*, 40(2004), No. 3, p. 225.

[8] P.F. Zuo, Comprehensive utilization of coal gangue, *Coal Technol.*, 28(2009), No. 1, p. 186.

[9] Y.X. Yan, X.F. Wang, and X.Q. Wang, Environmental effect and comprehensive utilization of coalmine waste from Huaibei and Huainan coalfield, *J. Anhui. Univ. Sci. Technol. Nat. Sci.*, 26(2006), No. 2, p. 9.

[10] D.H. Deng and W.L. Cen, Environmental effect of coal gangue stack area, *China Min. Magaz.*, (1999), No. 6, p. 87.

[11] F. Pan, X.C. Lu, T.Z. Wang, Y. Wang, Z.M. Zhang, Y. Yan, and S.P. Yang, Synthesis of large-mesoporous γ-Al_2O_3 from coal-series kaolin at room temperature, *Mater. Lett.*, 91(2013), p. 136.

[12] B.K. Wang, H. Ding, and Y.X. Deng, Characterization of calcined kaolin/TiO_2 composite particle material prepared by mechano-chemical method, *J. Wuhan. Univ. Technol. Mater. Sci. Ed.*, 25(2010), No. 5, p. 765.

[13] Y. Wen, N. Li, and B.Q. Han, Preparation and characterization of porous ceramics prepared by kaolinite gangue and $Al(OH)_3$ with double addition of $MgCO_3$ and $CaCO_3$, *Int. J. Miner. Metall. Mater.*, 18(2011), No. 4, p. 450.

[14] H.H. Murray, *Applied Clay Mineralogy*: *Occurrences*, *Processing, and Application of Kaolins*, *Bentonites*, *Palygorskite-sepiolite, and Common Clays*, Elsevier, 2007.

[15] H.F. Cheng, Q.F. Liu, J. Yang, and R.L. Frost, Thermogravimetric analysis of selected coal-bearing strata kaolinite, *Thermochim. Acta*, 507-508(2010), p. 84.

[16] S. Chandrasekhar and S. Ramaswamy, Influence of mineral impurities on the properties of kaolin and its thermally treated products, *Appl. Clay Sci.*, 21(2002), No. 3-4, p. 133.

[17] C.S. Zhu, J.H. Luan, P.H. Zhang, R.A. Huang, D. Liu, X.J. Xiang, and Z.N. Li, A study on calcinated whitening technology of kaolin in Benxi formation, Jiaozuo area, *Coal Geol. China*, 20(2008), No. 9, p. 14.

[18] E. Gámiz, M. Melgosa, M. Sánchez-Marañón, J.M. Martín-García, and R. Delgado, Relationships between chemico-mineralogical composition and color properties in selected natural and calcined Spanish kaolins, *Appl. Clay Sci.*, 28(2005), No. 1-4, p. 269.

[19] A. Martínez-Luévanos, M.G. Rodríguez-Delgado, A. Uribe-Salas, F.R. Carrillo-Pedroza, and J.G. Osuna-Alarcón, Leaching kinetics of iron from low grade kaolin by oxalic acid solutions, *Appl. Clay Sci.*, 51(2011), No. 4, p. 473.

[20] P.S. Sidhu, R.J. Gilkes, R.M. Cornell, A.M. Posner, and J.P. Quirk, Dissolution of iron oxides and oxyhydroxides in hydrochloric and perchloric acids, *Clays Clay Miner.*, 29(1981), No. 4, p. 269.

[21] M.A. Shabani, M. Irannajad, and A.R. Azadmehr, Investigation on leaching of malachite by citric acid, *Int. J. Miner. Metall. Mater.*, 19(2012), No. 9, p. 782.

[22] V.R. Ambikadevi and M. Lalithambika, Effect of organic acids on ferric iron removal from iron-stained kaolinite, *Appl. Clay Sci.*, 16(2000), No. 3-4, p. 133.

[23] F. Larroyd, C.O. Petter, and C.H. Sampaio, Purification of north Brazilian kaolin by selective flocculation, *Miner. Eng.*, 15(2002), No. 12, p. 1191.

[24] L.Z. Chen, G.P. Liao, Z.H. Qian, and J. Chen, Vibrating high gradient magnetic separation for purification of iron impurities under dry condition, *Int. J. Miner. Process.*, 102-103(2012), p. 136.

[25] C.T. Yavuz, A. Prakash, J.T. Mayo, and V.L. Colvin, Magnetic separations: from steel plants to biotechnology, *Chem. Eng. Sci.*, 64(2009), No. 10, p. 2510.

[26] R.M. Cornell and U. Schwertmann, *The Iron Oxides: Structure, Properties, Reactions, Occurrences and Uses*, VCH Publishers, New York, USA, 2003, p. 175.

[27] W. Künding, A least square fit program, *Nucl. Instrum. Methods*, 75(1969), No. 2, p. 336.

[28] G.P. Huffman and F.E. Huggins, Mössbauer studies of coal and coke: quantitative phase identification and direct determination of pyritic and iron sulphide sulphur content, *Fuel*, 57(1978), No. 10, p. 592.

[29] C.C. Hinckley, G.V. Smith, H. Twardowska, M. Saporoschenko, R.H. Shiley, and R.A. Griffen, Mössbauer studies of iron in Lurgi gasification ashes and power plant fly and bottom ash, *Fuel*, 59(1980), No. 3, p. 161.

[30] S.P. Taneja and C.H.W. Jones, Mössbauer studies of iron-bearing minerals in coal and coal ash, *Fuel*, 63(1984), No. 5, p. 695.

[31] L.C. Ram, P.S.M. Tripathi, and S.P. Mishra, Mössbauer

spectroscopic studies on the transformations of iron-bearing minerals during combustion of coals: Correlation with fouling and slagging, *Fuel Process. Technol.*, 42(1995), No. 1, p. 47.

[32] C.C. Zhou, G.J. Liu, Z.C. Yan, T. Fang, and R.W. Wang, Transformation behavior of mineral composition and trace elements during coal gangue combustion, *Fuel*, 97(2012), p. 644.

[33] C.E. White, J.L. Provis, T. Proffen, D.P. Riley, and J.S.J. van Deventer, Combining density functional theory (DFT) and pair distribution function (PDF) analysis to solve the structure of metastable materials: the case of metakaolin, *Phys. Chem. Chem. Phys.*, 12(2010), p. 3239.

[34] S.O. Lee, T. Tran, Y.Y. Park, S. J. Kim, and M.J. Kim, Study on the kinetics of iron oxide leaching by oxalic acid, *Int. J. Miner. Process.*, 80(2006), No. 2-4, p. 144.

[35] O. Castelein, L. Aldon, J. Olivier-Fourcade, J.C. Jumas, J.P. Bonnet, and P. Blanchart, ^{57}Fe Mössbauer study of iron distribution in a kaolin raw material: influence of the temperature and the heating rate, *J. Eur. Ceram. Soc.*, 22(2002), No. 11, p. 1767.